Hydrogen bonding described through diatomics-in-ionic-systems: The HF dimer

B. L. Grigorenko and A. V. Nemukhin
Department of Chemistry, Moscow State University, Moscow, 119899, Russian Federation

V. A. Apkarian
Department of Chemistry, University of California, Irvine, California 92697-2025

(Received 6 October 1997; accepted 15 December 1997)

With the proper inclusion of ion-pair configurations, the diatomics-in-molecules formalism can be used to accurately describe hydrogen bonding. This is demonstrated for the well characterized prototype, the HF dimer, the structure and entire potential energy surface of which is reproduced within its known accuracy: At the stationary points (potential minimum and saddle points) energies and bond lengths are reproduced with an accuracy of $\sim 1\%$, and the soft hydrogen bond angles are determined to within $\sim 5\%$. This is accomplished through a minimal basis Hamiltonian—19-dimensional matrix to describe the planar complex—constructed with analytic fits to accurately known or determined pair potentials. The construct includes the H^+F^- ion-pair states of the HF monomer units. The three-body nature of the inductive ion-pair interactions with neutrals is preserved, in the spirit of diatomic-in-ionic-systems. Based on *ab initio* estimates, in the limited range of interest, a Gaussian function describes the mixing between ionic and neutral states. The amplitude of this function is the only adjustable parameter in the model. The ionicity anisotropy and nonadditivity of interactions, responsible for the structure of the HF dimer, result naturally from mixing between ionic and neutral surfaces. © *1998 American Institute of Physics.*
[S0021-9606(98)02411-8]

I. INTRODUCTION

The semiempirical diatomics-in-molecules (DIM) theory,[1] originally developed to construct potential energy surfaces of polyatomics based solely on fragment diatomic interactions as input, is a well established formalism which has been successfully implemented in a variety of applications.[1–3] The formalism is particularly suited for reactive dynamics calculations, over ground and excited electronic surfaces, where efficient evaluation of realistic global potential energy surfaces are crucial;[2,3] and has been successful in applications to molecular structure determination.[4] A rather complete citation of the early work can be found in the review article by Kuntz.[3(c)] More recently, DIM has found utility in the description of intermolecular interactions, to describe anisotropies and nonadditivities in such, with the expressed purpose of developing a systematic approach to the description of multibody interactions, such as encountered in condensed media.[5–8] An illustrative example of the power and promise of the approach in such applications can be found in the recent simulations of nonadiabatic dynamics of I_2 and I_2^- in condensed media, simulations which included the full manifold of electronic states that correlate with $I(^2P_{1/2}, ^2P_{3/2})$ limits.[9]

In DIM, the choice of atomic configurations to be included determines the set of polyatomic basis functions (PBF) and their decomposition in terms of diatomic potentials. There is not a firm prescription for such a choice and hence for its partitioning. The guidance and constraints are provided by the aims of using the minimal basis set that retains the chemical insights at the desired level of rigor and accuracy. Through stringent requirements of spin coupling schemes and spatial transformations of directional atomic bases, DIM Hamiltonians reproduce the effects of valence, bond directionality, and configuration interaction.[1–3] When in addition to neutrals, ionic configurations are included, then configuration interaction between ionic and neutral states of the same symmetry produce the effects of polarization, or of bond ionicity. This aspect has been well recognized in the past. A good case study is the construction of the $O+H_2$ reactive surface, where it has been demonstrated that incorporation of the $O–H^+$, and $H^+–O^=–H^+$, configurations are crucial in generating realistic surfaces that contain the proper physics.[10] Moreover, once this important configuration is included, much of the excited states can be ignored and DIM matrices of manageable dimension can be produced to describe the global surfaces. Very closely related to the present study are DIM treatments of the $H+F_2$,[11] $F+HF$,[12,13] and $F+F_2$,[14] reactive surfaces, in which ionic contributions from H^+ and F^- fragments have been included. These treatments, however, suffer from the limitation that the inclusion of ionic states is made with strict adherence to DIM, treating all interactions as pairwise. The closely related formalism of diatomics-in-ionic-systems (DIIS),[15] evolved from the consideration of condensed phase systems, such as the charge transfer states of a Cl atom isolated in the polarizable lattice of Xe.[11(a),11(b)] A main difference in these treatments is the recognition that ionic interactions, and in particular induction terms, are vectorial multibody terms that

have to be incorporated as such. In essence, DIIS is not strictly a diatomics based method.[15] While the need for a consistent treatment of electrostatics in extended ionic systems is rather obvious, more subtle are the ''nonbonded'' interactions of small systems such as HF–Ar,[6(a)] and Cl_2–Ar,[6(c)] in which dispersion may be expected to be the dominant force. Yet, we have shown that the known nonadditivity of interactions in these cases can be retrieved through DIM matrices of reduced dimensionality, by ignoring much of the covalent electronic manifold while retaining in the construct a proper account of the energetics of the lowest ion-pair configurations: H^+F^- and Cl^+Cl^-, in these particular cases.[6(a),6(c)] As in DIIS, the three-body correction for an ion-pair interacting with a polarizable neutral was included in these treatments. The obvious implication of that analysis is that polarization plays a major role in the nonadditivity of pair potentials in these ''van der Waals'' complexes, and that these effects can be rather directly reproduced through configuration interaction between ionic and neutral states.

A natural extension of the above concepts and analysis is the consideration of hydrogen bonding. Given the ubiquity of hydrogen bonds and their importance in nature, a simple, accurate and insightful method of describing them should be valuable. We focus on the HF dimer, which as the prototype of H bonding has been extensively scrutinized by experiment, and by *ab initio* and semiempirical theories.[16–25] At present, the multidimensional potential energy surface of $(HF)_2$ is one of the best characterized, therefore, well suited as a test case. We give a systematic construct of the DIM potential surface, and compare it with other determinations. While previously we had been satisfied with qualitative descriptions of nonbonded interactions,[6] in the present case, we show that quantitatively accurate results are obtained. We surmise that this will not be limited to the case at hand. Having established the accuracy of the reproduced PES, we dissect various terms in the DIM matrix to provide an intuitive understanding of the subtleties of structure and couplings in this system. It should also be recognized that the surfaces by construct are global in nature, valid in regions where experiments have not yet probed. Accordingly, we provide the necessary details to lend the constructed matrix useful for dynamical calculations on this system.

The organization of this paper is as follows. Section II gives the essentials of the theory in its application to $(HF)_2$. Specification of the blocks for the DIM matrices is clarified in Appendix A. Diatomic fragment data are discussed in Sec. III, and the corresponding analytical functions are collected in Appendix B. The principles of neutral-ionic mixing applied here are discussed in Sec. IV. The results of the present calculations are given and discussed in Sec. V, where we compare the derived potential energy surface of $(HF)_2$ with the benchmark Quack–Suhm SQSBDE fit.[18] We close with concluding remarks in Sec. VI.

II. THE NEUTRAL-IONIC MODEL OF $(HF)_2$

The designations and geometric parameters of the $(HF)_2$ complex are shown in Fig. 1. We distinguish the bound F_bH_b and free F_fH_f monomer subunits, and the choice of angles

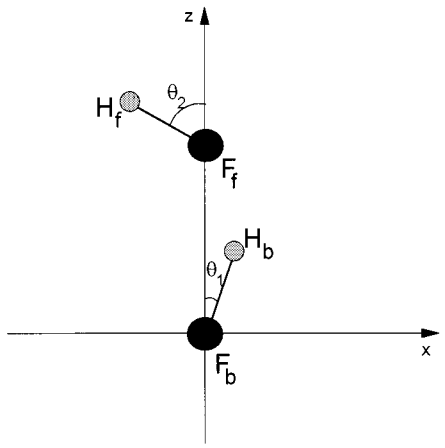

FIG. 1. Geometry of $(HF)_2$.

for in-plane rotations θ_1, θ_2 as indicated in Fig. 1. Although the matrices are initially constructed in full dimensionality, since the most important stationary points of the surface are contained in the planar geometry, we will restrict the evaluations to this plane.

The DIM formalism is nicely documented in many papers, we follow the matrix formulation originally given by Tully.[2] Quite generally, the polyatomic Hamiltonian operator may be partitioned into diatomic and monatomic parts[1]

$$\mathbf{H}=\sum_a \sum_{b>a} \mathbf{H}_{ab}-(N-2)\sum_a \mathbf{H}_a . \tag{1}$$

With the selected set of PBF's this Hamiltonian is converted into the matrix form, and the total Hamiltonian matrix whose eigenvalues give estimates of the polyatomic energies is decomposed into diatomic and monatomic matrices as prescribed by Eq. (1). The fragment matrices are constructed from the monatomic $\mathbf{V}_a$ and diatomic $\mathbf{V}_{ab}$ energies which are assumed to be known. The creation of monoatomic matrices requires only a knowledge of atomic energy levels, ionization potentials, and electron affinities. The construction of the diatomic part is more cumbersome. For each diatomic constituent, the initial basis set should be transformed in such a manner that the specific electronic states with respect to the spatial and spin quantum numbers are recognized. This is accomplished through a set of transformation matrices

$$\mathbf{H}_{ab}=(\mathbf{R}_b^{ab})^+(\mathbf{R}_a^{ab})^+\mathbf{T}_{ab}^+\mathbf{B}_{ab}^{-1}\mathbf{V}_{ab}\mathbf{B}_{ab}\mathbf{T}_{ab}\mathbf{R}_a^{ab}\mathbf{R}_b^{ab}, \tag{2}$$

in which $\mathbf{R}_a^{ab}$ represents the spatial rotation matrix that rotates the atomic quantization axis to the ab direction, $\mathbf{T}_{ab}$ is the spin transformation matrix of the fragment, and $\mathbf{B}_{ab}$ are the matrices which mix diatomic states.

Depending on the diatomic states concerned, $\mathbf{B}_{ab}$ will serve two different purposes. In the case of the heteronuclear HF fragments, the $\mathbf{B}_{ab}$ matrix connects states of the same spatial and spin symmetry. In our limited bases, the mixing in HF is only between two states: the $^1\Sigma^+$ ground state correlating with the lowest energy dissociation limit of neutral

TABLE I. Atomic states contributing to polyatomic basis functions and corresponding diatomic potentials.

	Diatomic potentials		
Atomic states	HF	H_2	$\mathbf{F_2}$
$F(^2P)H(^2S)F(^2P)H(^2S)$ 18 compositions	$^{1,3}\Sigma(HF),^{1,3}\Pi(HF)$	$^{1,3}\Sigma(H_2)$	$\chi\ ^1\Sigma_g^+,2\ ^1\Sigma_g^+,^1\Sigma_u^-,^1\Pi_g,^1\Pi_u,^1\Delta_g$ $1\ ^3\Sigma_u^+,2\ ^3\Sigma_u^+,^3\Sigma_g^-,^3\Pi_g,^3\Pi_u,^3\Delta_u$ all states of the F_2 fragment
$F^-(^1S)H^+F(^2P)H(^2S)$ $F(^2P)H(^2S)F^-(^1S)H^+$ $F^-(^1S)H(^2S)F(^2P)H^+$ $F(^2P)H^+F^-(^1S)H(^2S)$ 12 compositions	$^1\Sigma(H^+F^-)$, $^2\Sigma(HF^-),^2\Pi(H^+F)$, $^1\Sigma(HF),^1\Pi(HF)$	$^2\Sigma(H_2^+)_{g,u}$	$^2\Sigma(F_2^-)_{g,u},^2\Pi(F_2^-)_{g,u}$
$H^+F^-(^1S)H^+F^-(^1S)$ 1 term	$\begin{cases}^1\Sigma(H^+F^-) \text{ at } r_{HF}\approx r_{eq}\\ -1/r, \text{ otherwise}\end{cases}$	$1/r$	$1/r$

atoms $F(^2P)+H(^2S)$, and the ionic $^1\Sigma^+$ state correlating with the $F^-(^1S)+H^+$ limit. Accordingly, the needed 2×2 blocks $\mathbf{b}_{HF}$ of the unitary matrix $\mathbf{B}_{HF}$ are

$$\mathbf{b}_{HF}=\begin{pmatrix}\sin\beta(r_{HF}) & \cos\beta(r_{HF})\\ -\cos\beta(r_{HF}) & \sin\beta(r_{HF})\end{pmatrix}. \tag{3}$$

The mixing parameter β, which depends on the H–F distance, serves as the only adjustable parameter of the present model. Its evaluation will be described in Sec. IV. We should note here that the power of the DIM method is to a large extent grounded in the ambiguity of mixing parameter(s), which are allowed to be adjusted at some reference points on the polyatomic potential energy surface, and then used for predictions elsewhere. The ambiguity arises from the fact that, invariably, truncated bases are used for the decomposition. The strategy is, however, workable as long as the definitions are soundly grounded in theory. The choice of the elements of $\mathbf{B}_{HF}$ will be based on results of quantum chemistry calculations and the known experimental dissociation energy of $(HF)_2$. In the case of the homonuclear fragments, H_2 and F_2, the matrix $\mathbf{B}_{ab}$ unmixes the u and g states of the diatomic, i.e., states symmetrized with respect to inversion within the homonuclear fragment.

Table I shows the overall construct of the polyatomic basis functions and lists the electronic states of diatomic fragments HF, H^+F^-, HF^-, H^+F, F_2, F_2^- used to fill in the diagonal matrices $\mathbf{V}_{ab}$. In Appendix A we provide more explicit details of the matrix, and its block factorization in A' and A'' symmetries when the treatment is limited to the planar geometry.

Each of the basis functions shown in Table I is written as a product of atomic S functions or the Cartesian components of P functions multiplied by the proper spin factors. In the case of homonuclear diatomics these functions are transformed to relate them to molecular states of either g or u symmetry. This transformation is trivial for the S combinations required in the case of the H_2^+ fragment. In the case of P combinations, required for F_2 and F_2^- fragments, the procedure is direct and has previously been given explicitly by Gersonde and Gabriel in their treatment of the singlet states of diatomic halogens.[26] The same applies for the triplet states. The corresponding blocks of the matrices $\mathbf{B}_{A_2}^{-1}\cdot\mathbf{V}_{A_2}\cdot\mathbf{B}_{A_2}$, where A_2 stands for H_2^+, F_2, F_2^-, are given in Appendix A, and should be compared to the closely related matrices of $H+F_2$ and $F+F_2$ given by Duggan and Grice.[11,14]

As it is clear from Table I, which shows only S- and P-type atomic functions, the rotation matrices $\mathbf{R}_a^{ab}$ are easily constructed from the unit blocks and the 2×2 blocks of planar rotations with angles deduced from geometric considerations (see Fig. 1). Spin transformation matrices $\mathbf{T}_{ab}$ can also be obtained unambiguously, to generate singlet $(HF)_2$ from the definite spin states (singlet or triplet) of monomer subunits F_bH_b and F_fH_f. The required 2×2 blocks of the $\mathbf{T}$ matrices are also given in Appendix A.

The final expressions for the diatomic Hamiltonian matrices are

$$\begin{aligned}
\mathbf{H}_{H_bF_b}&=(\mathbf{R}_{F_b}^{H_bF_b}(\theta_1))^+\mathbf{B}_{HF}^{-1}\mathbf{V}_{H_bF_b}\mathbf{B}_{HF}\mathbf{R}_{F_b}^{H_bF_b}(\theta_1),\\
\mathbf{H}_{H_fF_f}&=(\mathbf{R}_{F_f}^{H_fF_f}(\theta_2))^+\mathbf{B}_{HF}^{-1}\mathbf{V}_{H_fF_f}\mathbf{B}_{HF}\mathbf{R}_{F_f}^{H_fF_f}(\theta_2),\\
\mathbf{H}_{H_fF_b}&=\mathbf{T}_{H_fF_b}^+(\mathbf{R}_{F_b}^{H_fF_b}(\theta_3))^+\mathbf{V}_{H_fF_b}\mathbf{R}_{F_b}^{H_fF_b}(\theta_3)\mathbf{T}_{H_fF_b},\\
\mathbf{H}_{H_bF_f}&=\mathbf{T}_{H_bF_f}^+(\mathbf{R}_{F_f}^{H_bF_f}(\theta_3))^+\mathbf{V}_{H_bH_f}\mathbf{R}_{F_f}^{H_bF_f}(\theta_3)\mathbf{T}_{H_bFf},\\
\mathbf{H}_{H_bH_f}&=\mathbf{T}_{H_2}^+\mathbf{B}_{H_2}^{-1}\mathbf{V}_{H_2}\mathbf{B}_{H_2}\mathbf{T}_{H_2},\\
\mathbf{H}_{F_bF_f}&=\mathbf{T}_{F_2}^+\mathbf{B}_{F_2}^{-1}\mathbf{V}_{F_2}\mathbf{B}_{F_2}\mathbf{T}_{F_2},
\end{aligned} \tag{4}$$

in which the angles θ_3 and θ_4 are those between the z axis and the H_b-F_f and H_f-F_b directions, respectively.

The dimension of the DIM matrix in the selected basis is 31. This would allow the consideration of arbitrary geometries of the complex. Limiting ourselves to the planar ge-

ometry, and the ground electronic state of $^1A'$ symmetry, it is sufficient to consider the 19×19 block of the full matrix. The energy surfaces of $(HF)_2$ to be discussed below, are obtained as the lowest eigenvalue of this 19-dimensional Hamiltonian matrix. The structure of the matrix, with components of the basis set arranged in the order: neutral, mixed neutral-ionic, and pure ionic, is schematically illustrated in Appendix A. The coupling between the corresponding blocks of the total matrix is governed by the mixing parameter β. If $\beta=0$, the energy of $(HF)_2$ comes from the 10×10 block of neutral states, if $\beta=90°$, then pure ionic structure is assumed. Intermediate values of β produce neutral-ionic mixing.

We deviate from a strictly DIM implementation by respecting the three-body, vectorial, nature of an ion-pair interacting with a neutral. As in our previous applications, we make this correction for the leading electrostatic term of charge induced dipoles only.[6] Noting that this r^{-4} term is contained in ion-neutral pair potentials which are used as scalar functions, we correct for the ion-pair interactions with neutral centers by adding the cross-polarization term. In the present application, this correction term

$$\Delta V_{\rm ion}=\alpha_{\rm H}\frac{\mathbf{r}_{\rm F^-H}\mathbf{r}_{\rm H^+H}}{\mathbf{r}^3_{\rm F^-H}\mathbf{r}^3_{\rm H^+H}}+\alpha_{\rm F}\frac{\mathbf{r}_{\rm F^-P}\mathbf{r}_{\rm H^+E}}{\mathbf{r}^3_{\rm F^-F}\mathbf{r}^3_{\rm H^+F}} \tag{5}$$

is added to the diagonal elements of the neutral-ionic part of the Hamiltonian matrix (α stands for polarizability). The effect of this correction is most significant for configurations $F_b^-H_b^+\cdots F_fH_f$ and $F_bH_b\cdots F_f^-H_f^+$, where $(\cdots)$ represents a separation large compared to the bondlength in the bound or free unit. Note, the inclusion of Eq. (5) is what distinguishes the present formulation from a strictly DIM treatment, since in effect, triatomics are included in the partitioning. To be more precise, the treatment should be qualified as DIIS.[15]

III. THE FRAGMENT ENERGIES

The constituent fragment energies of the diatomic Hamiltonian matrices are obtained through high level *ab initio* quantum chemistry calculations with appropriate empirical corrections. From pilot DIM estimates, we determine which of the diatomic contributions play the most important role in predictions of the $(HF)_2$ energies within the required limits of polyatomic coordinates, and pay special attention to the specification of these potential curves.

Accurate solutions of the adiabatic electronic equations are known for the required states $^2\Sigma_g^+$, $^2\Sigma_u^+$ of H_2^+,[27] and $^1\Sigma_g^+$, $^3\Sigma_u^+$ of H_2.[28] These *ab initio* energy points[27,28] are used in conjunction with the known long-range C_4 parameter, and the parameters (B,ζ) in the exchange energy expression $V_{\rm exch}=\pm B\cdot r\cdot\exp(-\zeta\cdot r)$ for the H_2^+ terms.[29]

For the diatomic potentials of F_2, F_2^-, HF, HF^+, and HF^- species, the same level of accuracy cannot be expected from *ab initio* data, and appropriate empirical corrections are required to construct the potential curves. We use experimental values for the ionization potential of H, 13.6 eV, and electron affinity of F, 3.40 eV,[29] to describe dissociation limits. For F_2 and F_2^--diatomic fragments, the *ab initio* results in given in Refs. 30 and 31 are used to obtain the functional fits given in Appendix B.

In spite of the known good quality *ab initio* data for the HF and $HF^{+/-}$ states, we recompute these potentials because the results described in the literature were given only in graphical form.[32–35] For the ground state $X\ ^1\Sigma^+$ potential of HF, we combine the experimental RKR curve given for internuclear distances $0.85\ \text{Å}<r_{\rm HF}<1\ \text{Å}$,[36] with our calculations and fix the dissociation energy with the experimental value of 6.12 eV.[37] Almost all HF potential curves have been obtained using large-scale configuration interaction (CI) calculations with the help of the GAMESS program suite,[38] using the AO basis set given explicitly by Segal and Wolf.[32] For each electronic state, first, the solutions of the MCSCF equations (the full optimized reaction space (FORS) option of GAMESS) have been obtained, by including the orbitals 2σ–4σ, 1π, 2π in the active space and keeping the $1s$(F) orbital in the core. Then the CI calculations were performed by using the second-order CI option of GAMESS with the FORS optimized molecular orbitals and FORS reference configurations (total number of configuration state functions actually used in CI is 75 000–125 000). To some extent, this procedure is equivalent to the MRD-CI treatment of Refs. 34, 35. In the $^1\Sigma^+$ block of the HF problem we needed two lowest roots of the secular equation, the first corresponded to the $X\ ^1\Sigma^+$, the second to the ion-pair H^+F^- potential.

The same approach has been applied for the calculations of the $X\ ^2\Pi$ state of H^+F. The computed pictures of all these curves are found to be consistent with those described in the previous calculations.[32–35]

We did not find references on the calculations of the $^2\Sigma^+$ state of H^+F. The curve computed by us has a peculiar shape with a barrier separating the potential well from the dissociation limit. The final energy values used in the fitting procedure were computed with even a greater effort, namely, using the QCISD(T) option of GAUSSIAN-94 in conjunction with the AUG-cc-pVTZ basis set.[39] The computed parameters of this curve, the potential well and barrier, are consistent with the results of recent photoelectron spectral studies of HF.[40]

In order to construct the $X\ ^2\Sigma^+$ potential of HF^- we employ the results of Ref. 35 together with those of our calculations. As has been concluded in Ref. 35, after crossing the $X\ ^1\Sigma^+$(HF) curve when moving from the dissociation limit $H+F^-$ the most stable form of HF^- is a free-electron $HF+e$ state, possessing a potential curve which parallels quite closely that of the neutral ground state. In fact, for these distances, both curves should coincide completely in the basis set limit when the number of diffuse atomic orbitals is sufficiently large to describe the unbound electron. Therefore, to represent this anionic potential we combined two curves: at $r_{\rm HF}<1.4\ \text{Å}$ (which corresponds to a crossing point according to Ref. 35) we took the curve of the ground state of neutral HF, and at $r_{\rm HF}>1.4\ \text{Å}$ we use a curve calculated by us with the QCISD(T) option of GAUSSIAN-94 using the AUG-cc-pVTZ basis set.

The fit to all potentials of ionic nature ($HF^{+/-}$,H^+F^-) given in Appendix B takes into account the experimental

data for the polarizabilities of the corresponding neutral partners, as well as other long-range coefficients for the $^1\Sigma^+$ states of HF.[29]

IV. MIXING PARAMETER FOR NEUTRAL AND IONIC STATES OF HF

In this application, as in our previous treatments,[6] we consider the mixing coefficient $\beta(r)$ as an adjustable parameter. Thus, while the construct forms a qualitatively correct framework for energy estimates, quantitative results are obtained by this semi-empirical adjustment. Note, β determines the ionicity of the ground state surface as a function of coordinates in the $(HF)_2$ complex. It appears explicitly in the HF fragment matrix. In principle, both intra-molecular ion-pair states and intermolecular charge transfer states could be included. However, $\beta(r)$ has a strong r dependence, scaling as the overlap between electron–hole wave functions. As such, the dominant contribution of mixing between ionic and neutral states can be expected to arise from the intramolecular coupling. Accordingly, we only consider mixing within the F_bH_b and F_fH_f monomer units, and ignore it for the cross pairs F_bH_f and F_fH_b. Note, however, that although the mixing coefficients appear only in the monomer units, intermolecular charge transfer configurations appear through the exchange interactions implicit in the H_2^+ and F_2^- fragment matrices.

An initial estimate of $\beta(r)$ is derived from the analysis of the variationally obtained coefficients C_k of configuration state functions in the conventional configuration interaction (CI) method, however, built on the atom-localized orbitals. More specifically, we apply the transformation from the canonical molecular orbitals calculated by the Hartree–Fock method to the natural atomic orbitals (NAO) within Weinhold's natural bond orbital analysis.[41] The NAO allow a clear interpretation of ionicity. In the present case, for the HF molecule, we insert into the CI expansions a set of atom-localized orbitals labeled as core $1s$(F), lone pair orbitals $2p_x$, $2p_y$, $2p_z$ of F and $1s$(H) instead of the canonical 1σ–3σ, 1π orbitals.

Construction of CI is carried out in a manner consistent with the full optimized reaction space (or complete active space) option by distributing 8 valence electrons of the HF molecule over F($2s$,$2p$) and H($1s$) orbitals. With the NAO it is possible to recognize the configuration state functions that correspond to the H^+F^- ionic electronic configuration. When taking the ratio $C_{\rm ion}^2/C_{\rm ion}^2+\Sigma C_{\rm neut}^2$, where $C_{\rm ion}$ and $C_{\rm neut}$ are the variational coefficients of the ground state CI wave function, we obtain the required estimate of the weight of the ionic configuration. In essence, we analyze the ratios of coefficients in valence-bond-type wave functions.

The quantum chemistry calculations described above have been carried out using the triple-zeta basis set for the ground state of HF. In the relevant range of H–F distances, $0.9\ \text{Å} > r > 3.2\ \text{Å}$, the computed dependence of $\sin^2\beta$ on r fits the Gaussian form

$$\sin^2\beta = A\ \exp[-B(r-C)^2] \tag{6}$$

with parameters $A=0.538$, $B=1.48\ \text{Å}^{-2}$, and $C=0.92\ \text{Å}$. Accordingly, for the cross-pairs, F_fH_b (where $r>1.8\ \text{Å}$ at equilibrium) and F_bH_f (where $r>3.2\ \text{Å}$), complete neglect of mixing is justified. Thus, we include mixing only in the monomer units, H_fF_f and H_bF_b, and while we retain the form suggested by Eq. (6) we treat coefficient A of the equation as the single adjustable parameter of the model. The adjustment is made at a single point on the multidimensional PES, at the equilibrium structure of the dimer, to reproduce the experimental dissociation energy of the hydrogen bond, $D_e=1561\ \text{cm}^{-1}$.[25] This is accomplished by varying A until the minimum energy of the DIIS surface as a function of all coordinates—$R_{\rm FF}$, θ_1, θ_2, $R(H_bF_b)$, $R(H_fF_f)$—agrees with the reference value. The final value of $A=0.383$ is used in the rest of the calculations.

The adjusted mixing parameter β, which reflects the ionicity of the HF bond, is noticeably different in different treatments of polyatomic systems where HF enters as a diatomic fragment. The value of β reported by Duggan and Grice, in their treatment of HF_2,[11] is approximately twice smaller than the value found optimal in our analysis of $(HF)_2$. Similarly, in our previous analysis of Ar–HF,[6(a)] the value determined for β was considerably smaller than in the present. These differences do not reflect serious inconsistencies, but rather, demonstrate the sensitivity of the results to the diatomic input information used in these semi-empirical analysis. Different procedures for extracting β and different pair potentials are used in these analyses. Nevertheless, in all cases acceptable representations of DIM polyatomic surfaces are derived.

V. RESULTS AND DISCUSSION

The equilibrium structure of $(HF)_2$ is firmly established through a variety of experimental and theoretical analyses.[16–25] The structure is illustrated in Fig. 1, and determined by the parameters $R_{\rm FF}=2.72\ \text{Å}$, $\theta_1=10°$, $\theta_2=63°$. The equilibrium values of θ_1, θ_2, which are fairly representative of such intermolecular complexes,[42] is nontrivial to rationalize. Quite clearly, a subtle balance of forces occurs, and this should be possible to generalize in hydrogen bonding systems. In the particular case of the HF dimer, a refined six-dimensional potential energy surface has been constructed by Quack and Suhm.[18] This so-called SQSBDE surface is given analytically, and in addition to optimizing the surface in full dimensionality to reproduce high resolution vibration–rotation spectra, *ab initio* quantum chemistry points,[21] and hydrogen bond dissociation energies are used to refine parameters of the surface. We will use this surface as a reference in discussing the DIIS results.

The DIIS energies for planar $(HF)_2$ are obtained as the lowest root of the 19×19 Hamiltonian matrix described in Sec. II using the diatomic inputs described in Sec. III, and the pair functions collected in Appendix B. The predicted surface is illustrated as a contour map in Fig. 2, juxtaposed with the reference surface of Quack and Suhm.[18] These plots represent the topology of the surfaces as a function of θ_1 and θ_2, at the equilibrium F–F distance (same as Fig. 7 of Ref. 18). The two surfaces are remarkably similar in all features.

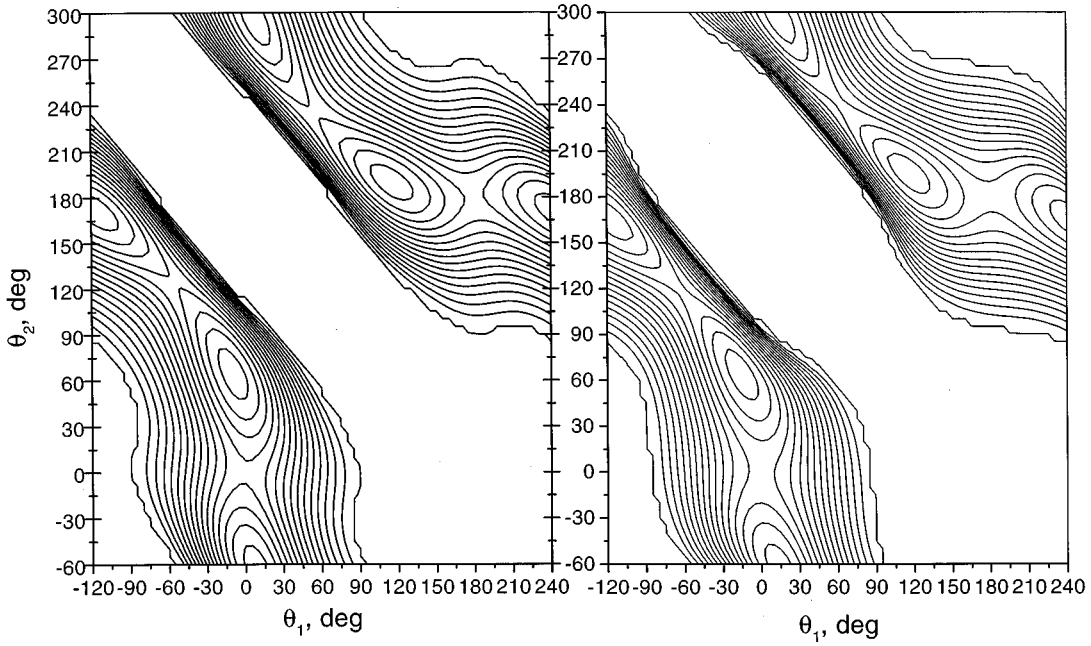

FIG. 2. 2D cuts of the DIM (left panel) and SQSBDE Ref. 18 (right panel) potential surfaces along θ_1 and θ_2 at the equilibrium F–F distance (contour lines are drawn every 100 cm^{-1} starting from 1600 cm^{-1}).

In Table II we compare the computed parameters of the three most important stationary points—the potential minimum, the C_{2h} saddle point, and the $C_{\infty v}$ saddle point—with those of the reference surface, as well as experimental and other theoretical determinations. It should be evident that in all comparisons the predictions are within the known accuracy of the features of this well determined surface.

At the C_s equilibrium geometry of the dimer, the deviation between our values and those of the reference surface, or experiment, is within the same limits as those computed with

TABLE II. Parameters of the stationary points of $(HF)_2$ (distances in Å, angles in degrees, energy in cm^{-1}).

Stationary point		$r_{(HF)_b}$	$r_{(HF)_r}$	R_{FF}	θ_1	θ_2	ΔE[a]
C_s minimum	This work	0.921	0.922	2.72	15	64	1560
	Quack & Suhm (Ref. 18)	0.923	0.921	2.722	9.0	64.13	1559.3
	Peterson & Dunning (Ref. 19)	0.922	0.920	2.73	7	69	1610
	Necoechea & Truhlar (Ref. 20)	0.923	0.921	2.723	9.9	65.47	1540.1
	Bunker *et al.* (Ref. 21)	0.922	0.922	2.749	7.1	61.7	1530
	Collins *et al.* (Ref. 22)	0.923	0.921	2.742	7.33	69.54	1655
	Experiment (Ref. 23)			2.72 ± 0.03	10 ± 6	63 ± 6	
	Experiment (Ref. 24)				7 ± 3	60 ± 2	
	Experiment[b]						1561
C_{2h} saddle							
	This work	0.921	0.921	2.640	62	118	332
	Quack and Suhm (Ref. 18)	0.922	0.922	2.629	54.92	125.08	351.5
	Necoechea, Truhlar (Ref. 20)	0.922	0.922	2.629	55.77	124.23	229.7
	Bunker *et al.* (Ref. 21)	0.923	0.922	2.722	56.1	123.9	332
$C_{\infty v}$ saddle							
	This work	0.920	0.921	2.83	0	0	297
	Quack and Suhm (Ref. 18)	0.923	0.920	2.815			333
	Bunker *et al.* (Ref. 21)	0.922	0.921	2.866			345

[a]ΔE for the minimum is the dissociation energy to two monomers HF+HF, ΔE for the saddle points are given with respect to the corresponding minimum energies.

[b]The experimental binding energies are derived from the D_0 of Bohac *et al.* (Ref. 25) and the zero-point vibrational corrections of Quack and Suhm (Ref. 18).

the help of large *ab initio* calculations. Within deviations of 0.1%, the DIIS values of the H–F distances show the effects of stretching from the original value of 0.917 Å in the uncomplexed molecule, with a slight asymmetry between bound and free units of the dimer. The F–F distance and θ_2 fall well within the uncertainties within which these quantities are known. The value of θ_1, showing deviation from the linear hydrogen bond axis, seems slightly overestimated in our results. This occurs in a very shallow basin, the contours of which seem in quite acceptable agreement with the reference surface (see Fig. 2).

Astonishing is the accuracy of the DIIS determination of the saddle points of the C_{2h} and $C_{\infty v}$ symmetry, particularly in view of the fact that the single adjustable parameter was fixed by the energy at the equilibrium geometry. The predictions for both geometry and energy of the saddle points are of comparative accuracy to the *ab initio* calculations. The determined bond lengths and energies at these points show the proper trends and remain within accuracy bars of $\sim 1\%$. Somewhat larger is the discrepancy of θ_1 and θ_2 at the C_{2h} saddle point when comparing the DIIS results with the other theoretical values. Again, these are soft coordinates, and the agreement should be regarded as surprisingly good.

Quite clearly, the present construct is capable in reproducing the subtle interplay of forces that determine the structure, energetics, and therefore presumably, the nature of hydrogen bonding.

Once the laborious task of constructing the DIIS matrix is completed, a major advantage of the formalism is that through the solution of algebraic equations entire surfaces are predicted. In particular, the scheme should lead to a correct description for every dissociation channel, since by construction all diatomic fragments dissociate into the correct limits, and therefore we know *a priori* that the energetics in asymptotic regions are true. We illustrate this feature by showing in Fig. 3 plots of the same surface for three increasing F–F distances, at 2.7, 4, and 6 Å. These surfaces then represent the adiabatic dissociation path of the complex into two monomer units. The constructed matrix should be quite useful in dynamical calculations.

Given the successful reproduction of structure and energetics, the investigation of contributions in our Hamiltonian that determine the final balance of interactions that dictate the HF dimer geometry, seems valuable. For example, the roles of neutral, ionic and mixed neutral-ionic terms in the Hamiltonian can be investigated by simply considering surfaces generated with the mixing parameter β set to 0°, 90°, and an intermediate value, respectively. We offer the following analysis.

The purely neutral model leads to the linear structure: F_b–$H_b\cdots F_f$–H_f with an exaggerated F–F distance extended to 3.7 Å and a binding energy of only 60 cm^{-1}. Evidently, the classical picture of a linear hydrogen bond arises from purely neutral contributions, and yields a binding energy characteristic of strictly dispersion interactions.

Deviations from linearity, which result from the anisotropy of intermolecular interactions, can only be explained when neutral-ionic mixing is taken into account ($0<\beta<90°$). The data of Table II and Figs. 2 and 3 are obtained

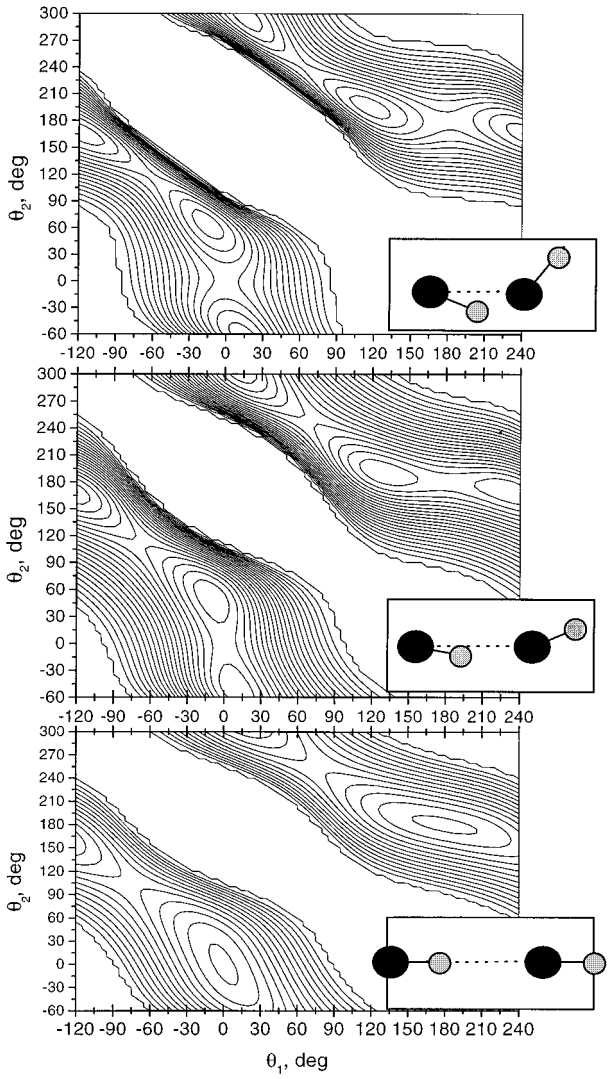

FIG. 3. 2D cuts of PES along θ_1 and θ_2 at (a) $R_{FF}=2.72$ Å (contour lines are drawn every 100 cm^{-1}, starting from 1600 cm^{-1}); (b) $R_{FF}=4$ Å (contour lines are drawn every 35 cm^{-1} starting from -525 cm^{-1}); (c) $R_{FF}=6$ Å (contour lines are drawn every 20 cm^{-1} starting from -140 cm^{-1}).

for $\beta\sim 38°$, at which value a significant admixture between ionic and neutral surfaces occurs. Therefore, in the present scheme, the asymmetry of the complex is *entirely* due to neutral-ionic mixing.

The mixed neutral-ionic block may be further decomposed to clarify the roles of specific diatomic potentials. To this end, the contour plots of Fig. 4 are informative. In these plots, the mixing parameter and the F–F distance are fixed at the equilibrium values of the full DIIS matrix, at 38°, and 2.7Å, respectively. The upper panel refers to the case when the ionic contributions from H_2^+ and F_2^- diatomics have been eliminated from the ionic block, and the corrections for the vectorial summation of the remaining ionic contributions [Eq. (5)] have been omitted. In sharp contrast with the linear arrangement of the purely neutral representation, the complex is now ''*L*'' shaped, with mutually orthogonal axes between bound and free monomers. This geometry is mainly

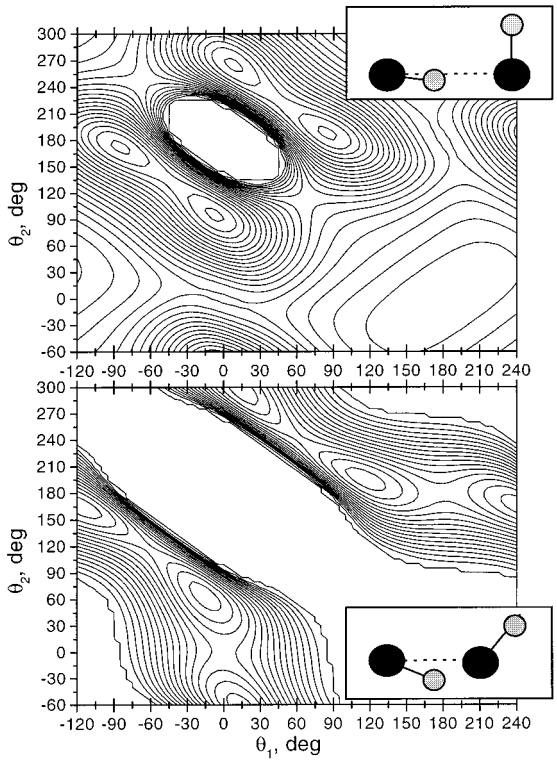

FIG. 4. 2D cuts for PES along θ_1 and θ_2 at $R_{FF}=2.72$ Å (contour lines are drawn every 100 cm^{-1}) and equilibrium structure computed with various contributions to the total potential (see the text).

determined by the contributions from the $^2\Pi$ and $^2\Sigma^+$ states of H^+F and from $^2\Sigma^+$ state of HF^-. Upon correcting for the three body ion-pair-atom interactions, by including the contribution from Eq. (5) the contour plot of the lower panel is obtained. This surface already shows the main features of the full treatment, and the predicted equilibrium structure is essentially the same as the final. We may therefore conclude that the delicate C_s equilibrium geometry of $(HF)_2$ is determined mainly by the $^2\Pi$ and $^2\Sigma^+$ states of HF^+ and $^2\Sigma^+$ state of HF^- and the three-body corrections to the ion-atom interactions. All other diatomic potentials, including intermolecular charge transfer configurations, play minor roles, but are necessary in obtaining the quantitative surface.

VI. CONCLUSIONS

By virtue of the accuracy with which the HF-dimer potential energy surface is known, it serves as a rigorous test for the adequacy of the DIIS method in quantitative treatments of hydrogen bonding. The success of the present treatment is highly encouraging. Given the construct of this semiempirical Hamiltonian, based on accurate pair potentials as input and a single adjustable parameter, we have little reason to doubt the generality of the result. Indeed, the approach used here is inspired by our prior success in treating HF–Ar and Cl_2–Ar and Cl_2–He complexes by the same method.[6] That work already indicated that a minimal DIIS basis of covalent states, augmented by a single ionic configuration in which three-body induction terms were properly included, was sufficient to reproduce the known nonadditivity of pair potentials. The necessity of including excited ionic configurations in DIIS matrices has a long history, with the main body of that work relying on coding the ionic contributions on a pairwise basis, in strict adherence with the DIM formalism. Neither in the case of the HF dimer, nor in the ''van der Waals'' clusters considered by us, would it be possible to account for the structural details and energetics based on pairwise interactions alone. Thus, as in the DIIS extension of DIM,[15] proper treatment of the electrostatic forces in the ionic states we regard as one the most important conclusions of the present quantitative test.

The peculiar structure of the HF dimer is nontrivial to rationalize by standard arguments. It arises from a subtle interplay between intermolecular forces. The structure arises naturally in our treatment, as a result of mixing between the anisotropic ionic excited state and the ground state. That the hydrogen bond is dominated by polarization is perhaps not too surprising. That the effect can be quantitatively reproduced by inclusion of the three-body, ion-pair induced polarization of the upper state, namely the leading electrostatic term in the ionic manifold, is an important finding. It suggests a general means for rationalizing such interactions, and a relatively direct method for constructing accurate surfaces. The required input for constructing such surfaces consists of a small set of diatomic pair potentials, atomic polarizabilities, and the mixing function between ionic and covalent potentials. The latter is treated as an adjustable parameter in the present. Given the important role the mixing function plays in these constructs, its systematics, and in particular its scaling with basis sets used, deserves more careful attention. Clearly, estimates of the mixing parameters can be obtained either from theory or from known polarities of bonds, and at that level already yield qualitatively correct surfaces. We should note that the model does not assume a fixed dipole on the HF monomers. Since the polarity of this bond is produced indirectly through mixing with the ionic surface, it is a flexible function of the geometry of the complex. This flexibility will appear as nonadditivity in intermolecular potentials created by electrostatic expansions.

Finally, we should admit that the accuracy with which the HF-dimer surface was reproduced, in particular the structure and energetics of the saddle points far from the minimum where the calibration was made, was surprising. Indeed the procedure involved the adjustment of one parameter, therefore remains semiempirical.

ACKNOWLEDGMENTS

We thank Dr. M. Suhm for sending us the FORTRAN codes of the SQSBDE surface. A MATHCAD PLUS 6.0 file for evaluation of the DIIS surfaces of HF dimer, with all necessary input parameters, is available from the authors upon request. This research was supported in part by the Russian Basic Research Foundation (Grant No. 96-03-32284) and in part through the U.S. Air Force Office of Scientific Research Grant No. F49620-1-0251.

TABLE III. The decomposition of the polyatomic basis set in terms of atomic functions, numbering of the PBF, and corresponding diatomic potentials that enter the V_{ab} matrices, for the $^1A'$ symmetry block.

	Atomic functions				Diatomic potentials				
N	H_b	F_b	H_f	F_f	$V(H_bF_b)$	$V(H_fF_f)$	$V(H_bF_f)$	$V(H_fF_b)$	$V(H_fH_b)$
1	$H(^2S)$	$F(^2P_x)$	$H(^2S)$	$F(^2P_x)$	$^1\Pi$	$^1\Pi$	$^1\Pi$	$^1\Pi$	$^1\Sigma$
2	$H(^2S)$	$F(^2P_x)$	$H(^2S)$	$F(^2P_x)$	$^3\Pi$	$^3\Pi$	$^3\Pi$	$^3\Pi$	$^3\Sigma$
3	$H(^2S)$	$F(^2P_x)$	$H(^2S)$	$F(^2P_z)$	$^1\Pi$	$^1\Sigma$	$^1\Sigma$	$^1\Pi$	$^1\Sigma$
4	$H(^2S)$	$F(^2P_x)$	$H(^2S)$	$F(^2P_z)$	$^3\Pi$	$^3\Sigma$	$^3\Sigma$	$^3\Pi$	$^3\Sigma$
5	$H(^2S)$	$F(^2P_y)$	$H(^2S)$	$F(^2P_y)$	$^1\Pi$	$^1\Pi$	$^1\Pi$	$^1\Pi$	$^1\Sigma$
6	$H(^2S)$	$F(^2P_y)$	$H(^2S)$	$F(^2P_y)$	$^3\Pi$	$^3\Pi$	$^3\Pi$	$^3\Pi$	$^3\Sigma$
7	$H(^2S)$	$F(^2P_z)$	$H(^2S)$	$F(^2P_x)$	$^1\Sigma$	$^1\Pi$	$^1\Pi$	$^1\Sigma$	$^1\Sigma$
8	$H(^2S)$	$F(^2P_z)$	$H(^2S)$	$F(^2P_x)$	$^3\Sigma$	$^3\Pi$	$^3\Pi$	$^3\Sigma$	$^3\Sigma$
9	$H(^2S)$	$F(^2P_z)$	$H(^2S)$	$F(^2P_z)$	$^1\Sigma$	$^1\Sigma$	$^1\Sigma$	$^1\Sigma$	$^1\Sigma$
10	$H(^2S)$	$F(^2P_z)$	$H(^2S)$	$F(^2P_z)$	$^3\Sigma$	$^3\Sigma$	$^3\Sigma$	$^3\Sigma$	$^3\Sigma$
11	H^+	$F^-(^1S)$	$H(^2S)$	$F(^2P_x)$	$^1\Sigma(H^+F^-)$	$^1\Pi$	$^2\Pi(H^+F)$	$^2\Sigma(HF^-)$	
12	$H(^2S)$	$F^-(^1S)$	H^+	$F(^2P_x)$	$^2\Sigma(HF^-)$	$^2\Pi(H^+F)$	$^1\Pi$	$^1\Sigma(H^+F^-)$	
13	H^+	$F^-(^1S)$	$H(^2S)$	$F(^2P_z)$	$^1\Sigma(H^+F^-)$	$^1\Sigma$	$^2\Sigma(H^+F)$	$^2\Sigma(HF^-)$	
14	$H(^2S)$	$F^-(^1S)$	H^+	$F(^2P_z)$	$^2\Sigma(HF^-)$	$^2\Sigma(H^+F)$	$^1\Sigma$	$^1\Sigma(H^+F^-)$	
15	H^+	$F(^2P_x)$	$H(^2S)$	$F^-(^1S)$	$^2\Pi(H^+F)$	$^2\Sigma(HF^-)$	$^1\Sigma(H^+F^-)$	$^1\Pi$	
16	$H(^2S)$	$F(^2P_x)$	H^+	$F^-(^1S)$	$^1\Pi$	$^1\Sigma(H^+F^-)$	$^2\Sigma(HF^-)$	$^2\Pi(H^+F)$	
17	H^+	$F(^2P_z)$	$H(^2S)$	$F^-(^1S)$	$^2\Sigma(H^+F)$	$^2\Sigma(HF^-)$	$^1\Sigma(H^+F^-)$	$^1\Sigma$	
18	$H(^2S)$	$F(^2P_z)$	H^+	$F^-(^1S)$	$^1\Sigma$	$^1\Sigma(H^+F^-)$	$^2\Sigma(HF^-)$	$^2\Sigma(H^+F)$	
19	H^+	$F^-(^1S)$	H^+	$F^-(^1S)$	$^1\Sigma(H^+F^-)$	$^1\Sigma(H^+F^-)$	$-1/r$	$-1/r$	$1/r$

APPENDIX A

Table I of the text shows the constituents of the polyatomic basis set of 31 functions used in the DIIS matrix. Tables III and IV give a more detailed description of the basis set and the diatomic inputs. There, we also number the PBF to describe the structure of the matrix. If we restrict ourselves to planar symmetry, then the 31×31 matrix can be blocked out into a 19×19 matrix of $^1A'$ symmetry and a 12×12 matrix of $^1A''$ symmetry. The $^1A''$ matrix consists of a 10×10, 8×8, and 1×1, blocks of neutrals, neutral-ionics, and ionic functions. Similarly, the $^1A''$ block consists of 8×8 and 4×4 blocks, of neutrals and neutral-ionics. This is also the ordering of the PBF vector in Tables III and IV.

The 2×2 spin transformation matrices: T_{ab} of Eq. (2), enter the neutrals block, along the diagonal, for the H_2, F_2, H_bF_f and H_fF_b fragments. They are

$$t_{H_bF_f}=t_{H_fF_b}=\begin{bmatrix} \frac{1}{2} & -\frac{\sqrt{3}}{2} \\ -\frac{\sqrt{3}}{2} & -\frac{1}{2} \end{bmatrix}, \tag{A1}$$

$$t_{H_2}=t_{F_2}=\begin{bmatrix} \frac{1}{2} & \frac{\sqrt{3}}{2} \\ \frac{\sqrt{3}}{2} & -\frac{1}{2} \end{bmatrix}. \tag{A2}$$

The F_2 fragment matrices appear in the neutrals as overlapping singlet and triplet manifolds (5×5 for $^1A'$ and 4×4 for $^1A''$). Explicitly

TABLE IV. The decomposition of the polyatomic basis set in terms of atomic functions, numbering of the PBF, and corresponding diatomic potentials that enter the V_{ab} matrices, for the $^1A''$ symmetry block.

	Atomic functions				Diatomic potentials				
N	H_b	F_b	H_f	F_f	$V(H_bF_b)$	$V(H_fF_f)$	$V(H_bF_f)$	$V(H_fF_b)$	$V(H_fH_b)$
20	$H(^2S)$	$F(^2P_x)$	$H(^2S)$	$F(^2P_y)$	$^1\Pi$	$^1\Pi$	$^1\Pi$	$^1\Pi$	$^1\Sigma$
21	$H(^2S)$	$F(^2P_x)$	$H(^2S)$	$F(^2P_y)$	$^3\Pi$	$^3\Pi$	$^3\Pi$	$^3\Pi$	$^3\Sigma$
22	$H(^2S)$	$F(^2P_y)$	$H(^2S)$	$F(^2P_x)$	$^1\Pi$	$^1\Pi$	$^1\Pi$	$^1\Pi$	$^1\Sigma$
23	$H(^2S)$	$F(^2P_y)$	$H(^2S)$	$F(^2P_x)$	$^3\Pi$	$^3\Pi$	$^3\Pi$	$^3\Pi$	$^3\Sigma$
24	$H(^2S)$	$F(^2P_y)$	$H(^2S)$	$F(^2P_z)$	$^1\Pi$	$^1\Sigma$	$^1\Sigma$	$^1\Pi$	$^1\Sigma$
25	$H(^2S)$	$F(^2P_y)$	$H(^2S)$	$F(^2P_z)$	$^3\Pi$	$^3\Sigma$	$^3\Sigma$	$^3\Pi$	$^3\Sigma$
26	$H(^2S)$	$F(^2P_z)$	$H(^2S)$	$F(^2P_y)$	$^1\Sigma$	$^1\Pi$	$^1\Pi$	$^1\Sigma$	$^1\Sigma$
27	$H(^2S)$	$F(^2P_z)$	$H(^2S)$	$F(^2P_y)$	$^3\Sigma$	$^3\Pi$	$^3\Pi$	$^3\Sigma$	$^3\Sigma$
28	H^+	$F^-(^1S)$	$H(^2S)$	$F(^2P_y)$	$^1\Sigma(H^+F^-)$	$^1\Pi$	$^2\Pi(H^+F)$	$^2\Sigma(HF^-)$	
29	$H(^2S)$	$F^-(^1S)$	H^+	$F(^2P_y)$	$^2\Sigma(HF^-)$	$^2\Pi(H^+F)$	$^1\Pi$	$^1\Sigma(H^+F^-)$	
30	H^+	$F(^2P_y)$	$H(^2S)$	$F^-(^1S)$	$^2\Pi(H^+F)$	$^2\Sigma(HF^-)$	$^1\Sigma(H^+F^-)$	$^1\Pi$	
31	$H(^2S)$	$F(^2P_y)$	H^+	$F^-(^1S)$	$^1\Pi$	$^1\Sigma(H^+F^-)$	$^2\Sigma(HF^-)$	$^2\Pi(H^+F)$	

$$
{}^1G=\begin{bmatrix}
\frac{2\,{}^1\Sigma_g^+ + {}^1\Delta_g}{2} & 0 & \frac{2\,{}^1\Sigma_g^+ - {}^1\Delta_g}{2} & 0 & 0 \\
0 & \frac{{}^1\Pi_g + {}^1\Pi_u}{2} & 0 & \frac{{}^1\Pi_u - {}^1\Pi_g}{2} & 0 \\
\frac{2\,{}^1\Sigma_g^+ - {}^1\Delta_g}{2} & 0 & \frac{2\,{}^1\Sigma_g^+ + {}^1\Delta_g}{2} & 0 & 0 \\
0 & \frac{{}^1\Pi_u - {}^1\Pi_g}{2} & 0 & \frac{{}^1\Pi_g + {}^1\Pi_u}{2} & 0 \\
0 & 0 & 0 & 0 & X\,{}^1\Sigma_g^+
\end{bmatrix}, \tag{A3}
$$

$$
{}^1G''=\begin{bmatrix}
\frac{{}^1\Delta_g + {}^1\Sigma_u^-}{2} & \frac{{}^1\Delta_g - {}^1\Sigma_u^-}{2} & 0 & 0 \\
\frac{{}^1\Delta_g - {}^1\Sigma_u^-}{2} & \frac{{}^1\Delta_g + {}^1\Sigma_u^-}{2} & 0 & 0 \\
0 & 0 & \frac{{}^1\Pi_g + {}^1\Pi_u}{2} & \frac{{}^1\Pi_u - {}^1\Pi_g}{2} \\
0 & 0 & \frac{{}^1\Pi_u - {}^1\Pi_g}{2} & \frac{{}^1\Pi_g + {}^1\Pi_u}{2}
\end{bmatrix}, \tag{A4}
$$

$$
{}^3G=\begin{bmatrix}
\frac{{}^3\Delta_u + {}^3\Sigma_g^-}{2} & 0 & \frac{{}^3\Delta_u - {}^3\Sigma_g^-}{2} & 0 & 0 \\
0 & \frac{{}^3\Pi_g + {}^3\Pi_u}{2} & 0 & \frac{{}^3\Pi_u - {}^3\Pi_g}{2} & 0 \\
\frac{{}^3\Delta_u - {}^3\Sigma_g^-}{2} & 0 & \frac{{}^3\Delta_u + {}^3\Sigma_g^-}{2} & 0 & 0 \\
0 & \frac{{}^3\Pi_u - {}^3\Pi_g}{2} & 0 & \frac{{}^3\Pi_g + {}^3\Pi_u}{2} & 0 \\
0 & 0 & 0 & 0 & 1\,{}^3\Sigma_u^+
\end{bmatrix}, \tag{A5}
$$

$$
{}^3G''=\begin{bmatrix}
\frac{2\,{}^3\Sigma_u^+ + {}^3\Delta_u}{2} & \frac{2\,{}^3\Sigma_u^+ - {}^3\Delta_u}{2} & 0 & 0 \\
\frac{2\,{}^3\Sigma_u^+ - {}^3\Delta_u}{2} & \frac{2\,{}^3\Sigma_u^+ + {}^3\Delta_u}{2} & 0 & 0 \\
0 & 0 & \frac{{}^3\Pi_g + {}^3\Pi_u}{2} & \frac{{}^3\Pi_u - {}^3\Pi_g}{2} \\
0 & 0 & \frac{{}^3\Pi_u - {}^3\Pi_g}{2} & \frac{{}^3\Pi_g + {}^3\Pi_u}{2}
\end{bmatrix}, \tag{A6}
$$

where the ${}^1G'$, ${}^1G''$, ${}^3G'$, and ${}^3G''$ matrices act on the PBF vectors [1, 3, 5, 7, 9], [21, 23, 25, 27], [2, 4, 6, 8, 10], [20, 22, 24, 26], respectively.

The H_2/H_2^+ fragment matrices enter the neutral-ionic blocks as 2×2 matrices

$$\begin{bmatrix} \frac{^2\Sigma_g^+ + ^2\Sigma_u^+}{2} & \frac{^2\Sigma_g^+ - ^2\Sigma_u^+}{2} \\ \frac{^2\Sigma_g^+ - ^2\Sigma_u^+}{2} & \frac{^2\Sigma_g^+ + ^2\Sigma_u^+}{2} \end{bmatrix} \tag{A7}$$

along the diagonal; and the following combinations of the F_2^- electronic states:

$$^2G'' = \begin{bmatrix} \frac{^2\Pi_g + ^2\Pi_u}{2} & 0 & 0 & 0 & \frac{^2\Pi_u - ^2\Pi_g}{2} & 0 & 0 & 0 \\ 0 & \frac{^2\Pi_g + ^2\Pi_u}{2} & 0 & 0 & 0 & \frac{^2\Pi_u - ^2\Pi_g}{2} & 0 & 0 \\ 0 & 0 & \frac{^2\Sigma_g + ^2\Sigma_u}{2} & 0 & 0 & 0 & \frac{^2\Sigma_g - ^2\Sigma_u}{2} & 0 \\ 0 & 0 & 0 & \frac{^2\Sigma_g + ^2\Sigma_u}{2} & 0 & 0 & 0 & \frac{^2\Sigma_g - ^2\Sigma_u}{2} \\ \frac{^2\Pi_u - ^2\Pi_g}{2} & 0 & 0 & 0 & \frac{^2\Pi_g + ^2\Pi_u}{2} & 0 & 0 & 0 \\ 0 & \frac{^2\Pi_u - ^2\Pi_g}{2} & 0 & 0 & 0 & \frac{^2\Pi_g + ^2\Pi_u}{2} & 0 & 0 \\ 0 & 0 & \frac{^2\Sigma_g - ^2\Sigma_u}{2} & 0 & 0 & 0 & \frac{^2\Sigma_g + ^2\Sigma_u}{2} & 0 \\ 0 & 0 & 0 & \frac{^2\Sigma_g - ^2\Sigma_u}{2} & 0 & 0 & 0 & \frac{^2\Sigma_g + ^2\Sigma_u}{2} \end{bmatrix}, \tag{A8}$$

$$^2G'' = \begin{bmatrix} \frac{^2\Pi_g + ^2\Pi_u}{2} & 0 & \frac{^2\Pi_u - ^2\Pi_g}{2} & 0 \\ 0 & \frac{^2\Pi_g + ^2\Pi_u}{2} & 0 & \frac{^2\Pi_u - ^2\Pi_g}{2} \\ \frac{^2\Pi_u - ^2\Pi_g}{2} & 0 & \frac{^2\Pi_g + ^2\Pi_u}{2} & 0 \\ 0 & \frac{^2\Pi_u - ^2\Pi_g}{2} & 0 & \frac{^2\Pi_g + ^2\Pi_u}{2} \end{bmatrix}. \tag{A9}$$

APPENDIX B

Analytic formulas used for diatomic potentials (distances in Å, energies in eV).

H_2:

$$^1\Sigma_g^+(H_2): 12.72 \cdot e^{-3.2806\cdot(r-0.74)} - 17.47 \cdot e^{-2.3911\cdot(r-0.74)}$$

$$^3\Sigma_u^+(H_2): 38.38 \cdot e^{-2.4934\cdot r}$$

$$^2\Sigma_g^+(H_2^+): 6.447 \cdot e^{-3.6673\cdot r} \cdot \left(\frac{1}{r^5} + 96.20 - 123.84 \cdot r + 73.75 \cdot r^2\right) - 37.85 \cdot r \cdot e^{-1.8904\cdot r} - \frac{4.795}{r^4}$$

$$^2\Sigma_u^+(H_2^+): 5.258 \cdot e^{-4.31\cdot r} \cdot \left(\frac{1}{r^5} + 206.52 - 246.67 \cdot r + 169.02 \cdot r^2\right) + 37.85 \cdot r \cdot e^{-1.8904\cdot r} - \frac{4.795}{r^4}$$

F_2:

$$^1\Sigma_g^+(F_2): -3.2 \cdot e^{-3.028\cdot(r-1.411)} + 1.6 \cdot e^{-6.056\cdot(r-1.411)}$$

$$^1\Pi_u(F_2): 8.62.108 \cdot e^{-4.1524\cdot r}$$

$$^1\Pi_g(F_2): 2272.784 \cdot e^{-4.2425\cdot r}$$

$$^1\Delta_g(F_2): 1242.653 \cdot e^{-3.6701\cdot r}$$

$$2\,^1\Sigma_g^+(F_2): 1278.363\cdot e^{-3.6539\cdot r}$$

$$^1\Sigma_u^-(F_2): 1779.913\cdot e^{-3.813\cdot r}$$

$$^3\Pi_u(F_2): 0.2465\cdot e^{-5.7277\cdot r(-1.88)} - 0.3977 \cdot e^{-3.4547\cdot (r-1.88)}$$

$$^3\Pi_g(F_2): 2050.589\cdot e^{-4.2609\cdot r}$$

$$1\,^3\Sigma_u^+(F_2): 1474.892\cdot e^{-3.9829\cdot r}$$

$$^3\Sigma_g^-(F_2): 1132.92\cdot e^{-3.6788\cdot r}$$

$$^3\Delta_u(F_2): 1757.222\cdot e^{-3.7951\cdot r}$$

$$2\,^3\Sigma_u^+(F_2): 1682.331\cdot e^{-3.7591\cdot r}$$

$$^2\Sigma_u^+(F_2^-): -5.648\cdot e^{-1.6745(r-1.411)} + 6.317 \cdot e^{-3.349\cdot (r-1.411)}$$

$$^2\Sigma_g^+(F_2^-): -0.854\cdot e^{-1.1506\cdot (r-1.411)} + 8.381 \cdot e^{-2.3013\cdot (r-1.411)}$$

$$^2\Pi_g(F_2^-): -0.8352\cdot e^{-1.4383\cdot (r-1.411)} + 3.298 \cdot e^{-2.8766\cdot (r-1.411)}$$

$$^2\Pi_u(F_2^-): -1.338\cdot e^{-1.2869\cdot (r-1.411)} + 6.162 \cdot e^{-2.5738\cdot (r-1.411)}$$

HF:

$$^1\Sigma^+(HF): \begin{cases} 8.464\cdot x^2 - 10.755\cdot x^3 + 9.301\cdot x^4 - 7.046\cdot x^5 + 3.444\cdot x^6 - 6.12, x = \dfrac{r-0.9169}{a_0}, & 0.85 < r_{HF} < 1\,\text{Å} \\ -63.738\cdot e^{-2.233\cdot r} + 5927.588\cdot e^{-7.2109\cdot r} - \dfrac{3.224}{r^6}, & r_{HF} > 1\,\text{Å} \end{cases}$$

$$^1\Sigma^+(H^+F): -1.692\cdot e^{-1.619\cdot r}\cdot\left(1 - 162.52\cdot r + 91.906\cdot r^2 - 14.649\cdot r^3 + \frac{129.73}{r} - \frac{111.92}{r^2}\right) - \frac{10.911}{r^4} - \frac{14.396}{r}$$

$$^3\Sigma(HF): 118.693\cdot e^{-2.904\cdot r}$$

$$^1\Pi(HF): 45.312\cdot e^{-2.4071\cdot r}$$

$$^3\Pi(HF): 52.12\cdot e^{-2.6856\cdot r}$$

$$^2\Sigma^+(H^+F): 4.327\cdot e^{-1.1159\cdot r} + 1208.06\cdot e^{-5.218\cdot r} - \frac{8.06}{r^4}$$

$$^2\Pi(H^+F): 5.159\cdot e^{-3.318\cdot r}\cdot(1 + 21.878\cdot r - 24.649\cdot r^2) + 2315.189\cdot e^{-6.191\cdot r} - \frac{8.06}{r^4}$$

$$^2\Sigma^+(HF^-): 13.998\cdot e^{-2.524\cdot r}\cdot(1 + 9.94\cdot r - 7.89\cdot r^2 + 1.71\cdot r^3) + 81725.976\cdot e^{-10.797\cdot r} - \frac{9.547}{r^4}.$$

[1] F. O. Ellison, J. Am. Chem. Soc. **85**, 3540 (1963).

[2] J. C. Tully, in *Modern Theoretical Chemistry, Semiempirical Methods of Electronic Structure Calculations*, edited by G. A. Segal (Plenum, New York, 1977), Vol. 7A, Chap. 6; J. C. Tully, in *Potential Energy Surfaces*, edited by K. P. Lawley (Wiley, New York, 1980), pp. 63–112.

[3] (a) P. J. Kuntz, in *Dynamics of Molecular Collisions*, edited by W. H. Miller, Part B (Plenum, New York, 1976), p. 53; (b) P. J. Kuntz, in *Atom–Molecule Collision Theory—A Guide for the Experimentalist*, edited by R. B. Bernstein (Plenum, New York, 1979), Chap. 3; (c) P. J. Kuntz, in *Theoretical Models of Chemical Bonding, Part 2, The Concept of the Chemical Bond*, edited by Z. B. Maksic (Springer, Berlin, 1980). pp. 321–376.

[4] (a) A. V. Nemukhin and N. F. Stepanov, Int. J. Quantum Chem. **15**, 49 (1979); (b) S. V. Ljudkovskii, A. V. Nemukhin, and N. F. Stepanov, J. Mol. Struct.: THEOCHEM **104**, 403 (1983).

[5] W. G. Lawrence, and V. A. Apkarian, J. Chem. Phys. **101**, 1820 (1994); A. V. Danilychev, and V. A. Apkarian, *ibid.* **100**, 5556 (1994).

[6] (a) B. L. Grigorenko, A. V. Nemukhin, and V. A. Apkarian, J. Chem. Phys. **104**, 5510 (1996); (b) B. L. Grigorenko, A. V. Nemukhin, A. A. Buchachenko, N. F. Stefanov, and S. Ya. Umanskii, *ibid.* **106**, 4575 (1997); (c) B. L. Grigorenko, A. V. Nemukhin, and V. A. Apkarian, Chem. Phys. **19**, 161 (1997), (d) A. V. Nemukhin, B. L. Grigorenko, and A. V. Savin, Chem. Phys. Lett. **250**, 226 (1996).

[7] A. A. Buchachenko and N. F. Stepanov, J. Chem. Phys. **104**, 9913 (1996).

[8] F. Yu. Naumkin, P. J. Knowles, and J. N. Murrell, Chem. Phys. **193**, 27 (1995); F. Yu. Naumkin and P. J. Knowles, J. Chem. Phys. **103**, 3392 (1995); F. Yu. Naumkin, Mol. Phys. **90**, 875 (1997).

[9] V. S. Batista and D. F. Coker, J. Chem. Phys. **105**, 4033 (1996); **106**, 7102, 6923 (1997).

[10] P. A. Berg, J. J. Sloan, and P. J. Kuntz, J. Chem. Phys. **95**, 8038 (1991); P. J. Kuntz, B. I. Neifer, and J. J. Sloan, *ibid.* **88**, 3629 (1988); R. Polak, I. Paidarova, and P. J. Kuntz, *ibid.* **87**, 2663 (1987); R. Polak, I. Paidarova, and P. J. Kuntz, *ibid.* **82**, 2352 (1985).

[11] J. J. Duggan and R. Grice, J. Chem. Phys. **78**, 3842 (1983).

[12] I. Last, Chem. Phys. **69**, 193 (1982).

[13] J. J. Duggan and R. Grice, J. Chem. Soc. Faraday Trans. **80**, 739 (1983).

[14] J. J. Duggan and R. Grice, J. Chem. Soc. Faraday Trans. **80**, 795 (1984).

[15] (a) I. Last and T. F. George, J. Chem. Phys. **87**, 1183 (1987); (b) I. Last, T. F. George, M. E. Fajardo, and V. A. Apkarian, *ibid.* **87**, 5917 (1987); (c) I. Last and T. F. George, *ibid.* **93**, 8925 (1990); **98**, 6406 (1993).

[16] D. G. Truhlar, in Proceedings of the NATO Workshop on the dynamics of polyatomic van der Waals Complexes, NATO Ser. B **227**, 159 (1990).

[17] M. Quack and M. A. Suhm, in *Conceptual Perspectives in Quantum Chemistry*, edited by J.-L. Calais and E. S. Kryachko, Vol. III of Conceptual Trends in Quantum Chemistry, 417 (Kluwer, Dordrecht, 1997).

[18] M. Quack and M. A. Suhm, J. Chem. Phys. **95**, 28 (1991).

[19] K. A. Peterson and T. H. Dunning, J. Chem. Phys. **102**, 2032 (1995).

[20] W. C. Necoechea and D. G. Truhlar, Chem. Phys. Lett. **248**, 182 (1996).

[21] P. R. Bunker, M. Kofranek, H. Lischka, and A. Karpfen, J. Chem. Phys. **89**, 3002 (1988).
[22] C. L. Collins, K. Morihashi, Y. Yamaguchi, and H. F. Schaefer III, J. Chem. Phys. **103**, 6051 (1995).
[23] B. J. Howard, T. R. Dyke, and W. Klemperer, J. Chem. Phys. **81**, 5417 (1984).
[24] H. S. Gutowsky, C. Chuang, J. D. Keen, T. D. Klots, and T. Emulsson, J. Chem. Phys. **83**, 2070 (1985).
[25] E. J. Bohac, M. D. Marshall, and R. E. Miller, J. Chem. Phys. **96**, 6681 (1992).
[26] I. H. Gersonde and H. Gabriel, J. Chem. Phys. **98**, 2094 (1993).
[27] J. M. Peek, J. Chem. Phys. **43**, 3004 (1965).
[28] W. Kolos and L. Wolniewicz, J. Chem. Phys. **43**, 2429 (1965).
[29] A. A. Radzig and B. M. Smirnov, *Handbook on Atomic and Molecular Physics* (Atomizdat, Moscow, 1980).
[30] D. C. Cartwright and P. J. Hay, J. Chem. Phys. **70**, 3191 (1979).
[31] J. G. Dojahn, E. C. M. Chen, and W. E. Wentworth, J. Chem. Phys. **100**, 9649 (1996).
[32] G. A. Segal and K. Wolf, Chem. Phys. **56**, 321 (1981).
[33] G. A. Segal and K. Wolf, J. Phys. B **14**, 2291 (1981).
[34] M. Bettendorf, R. J. Buenker, S. D. Peyerimhoff, and J. Roemelt, Z. Phys. A **304**, 125 (1982).
[35] M. Bettendorf, R. J. Buenker, and S. D. Peyerimhoff, Mol. Phys. **50**, 1363 (1983).
[36] D. W. Schwenke and D. G. Truhlar, J. Chem. Phys. **88**, 4800 (1988).
[37] K. P. Huber and G. Herzberg, *Molecular Spectra and Molecular Structure, IV. Constants of Diatomic Molecules* (Van Nostrand Reinhold, New York, 1979).
[38] M. W. Schmidt, K. K. Baldridge, J. A. Boatz, S. T. Elbert, M. S. Gordon, J. H. Jensen, S. Koseki, N. Matsunaga, K. A. Nguyen, S. J. Su, T. L. Windus, M. Dupuis, and J. A. Montgomery, J. Comput. Chem. **14**, 1347 (1993).
[39] GAUSSIAN 94, M. J. Frisch, G. W. Trucks, H. B. Schlegel, P. M. W. Gill, B. G. Johnson, M. A. Robb, J. R. Cheeseman, T. Keith, G. A. Petersson, J. A. Montgomery, K. Raghavachari, M. A. Al-Laham, V. G. Zakrzewski, J. V. Ortiz, J. B. Foresman, J. Cioslowski, B. B. Stefanov, A. Nanayakkara, M. Challacombe, C. Y. Peng, P. Y. Ayala, W. Chen, M. W. Wong, J. L. Andres, E. S. Replogle, R. Gomperts, R. L. Martin, D. J. Fox, J. S. Binkley, D. J. Defrees, J. Baker, J. P. Stewart, M. Head-Gordon, C. Gonzalez, and J. A. Pople (Gaussian, Inc., Pittsburgh, PA, 1995).
[40] D. Edvardsson, P. Baltzer, L. Karlsson, M. Lundquist, and B. Wannberg, J. Electron Spectrosc. Relat. Phenom. **73**, 105 (1995).
[41] A. E. Reed, L. A. Curtiss, and F. Weinhold, Chem. Rev. **88**, 899 (1988).
[42] P. Hobza and R. Zahradnik, *Intermolecular Complexes* (Elsevier, Amsterdam, 1988).